Y3.N21/5:8/826

M826

Hartford Public Library

TECHNICAL MEMORANDUMS

NATIONAL ADVISORY COMMITTEE FOR AERONAUTICS

No. 826

THE SCALE EFFECT IN TOWING TESTS WITH AIRPLANE-FLOAT SYSTEMS

By Rudolph Schmidt

Luftfahrtforschung
Vol. XIII, No. 7, July 20, 1936

Washington
May 1937

NATIONAL ADVISORY COMMITTEE FOR AERONAUTICS

TECHNICAL MEMORANDUM NO. 826

THE SCALE EFFECT IN TOWING TESTS WITH AIRPLANE-FLOAT SYSTEMS*

By Rudolph Schmidt

In the design of seaplanes it is necessary to know the manner in which the forces and moments on the float system vary in order to predict the take-off performance. As a rule the bases of the computations are the results of tests of models in a towing tank but the conversion of these to the full size shows deviations from the truth. The DVL accordingly developed a method for the determination of the forces and moments on full-size floats.

SUMMARY

The present report includes a description of the making of three-component measurements on a full-size float mounted on an actual airplane and the comparison of the results with those from two models of the same form but of different size which had been tested in the towing tank. The purpose of the comparison is to determine the effect of the Reynolds Number on the results of model tank tests.

The float was tested at three scales: at full size fitted to the seaplane itself with specially developed test equipment, and in 1:2.5 and 1:5 sizes in the Naval Research Laboratories at Hamburg and Berlin.

Following a brief discussion of previous tests intended to elucidate the problem of scale effect on float systems and a description of the testing equipment, the choice of the reference quantities to be used in the comparison is discussed. The selection of load, speed, and trim as a basis of comparison seems best suited to the

---

*"Der Masstabeinfluss beim Schleppversuch mit Flugzeug-Schwimmerken." Luftfahrtforschung, vol. XIII, no. 7, July 20, 1936, pp. 224-237.

practical operation of making this comparison. The quantities affected by scale are then: resistance, trimming moment, and their derivatives; planing number (resistance/weight on water); and position of center of pressure.

In order to assure a proper comparison at high speeds, the effect of the air forces on the exposed parts of the float must also be considered. This was done by means of a model test in the small DVL tunnel. The experimental part of the report closes with a discussion of the curves, their discrepancies, and the probable causes of the discrepancies.

The theoretical part gives an explanation of the concept "scale effect" as well as its physical causes. The scale effect is most conveniently analyzed by considering its effects on the tangential (friction) forces separately from those of the normal (pressure) forces. Based on the theoretically and experimentally determined laws for the coefficients of friction on plates in longitudinal flow, the methods in which both the Reynolds Number for the three sizes of model and the coefficients of friction for plates at the same Reynolds Number vary are investigated in a numerical example. The effect of the Reynolds Number on the trimming moment takes the form of a change in the pressure distribution as a result of the separation phenomena which may have a variety of causes. It was found that the method of influencing the pressure distribution and obtaining a better agreement between ship and model by means of a so-called "turbulence wire" used in tank tests of ship models is ineffectual on seaplane floats.

It is shown in a numerical example that the order of magnitude of the scale effect on both friction and pressure forces is in magnitude and direction in satisfactory accord with theory and with the results from tests of planing surfaces if the partially rough assumptions are taken into account. Extrapolating this result to the size of the largest flying boats built so far (Do X, with 48 tons total weight), it is observed that for the investigation of float systems of such enormous size it is necessary to choose a model scale for which the Reynolds Numbers correspond to those of the 1:2.5 scale model. The scale effect then is approximately 50 percent of the frictional resistance of the model.

Another example shows how the experimentally deter-

mined scale effect may affect the calculation of the take-off time and run in designs with different power loading. A favorable circumstance is that the resistance from the model test is always greater than for the full size and that consequently the take-off performances computed on the basis of model experiments will always be inferior to those of the actual seaplane.

The results are summarized as follows:

1. The measured scale effect is, on the whole, in satisfactory agreement with theory and with tests of plates and planing surfaces.

2. The use of the "turbulence wire" or roughening the surface is impracticable for tests of float systems.

3. The method of conversion customary in ship design is impracticable.

4. The calculation of take-off performances based on model tests leaves one on the safe side.

5. In order to make safe calculations in advance of take-off performances, it is necessary to use models of the order of the 1:2.5 scale comparative model.

The experiments described herein have been duplicated, using another family of models of a different form. The results were fundamentally the same.

I. INTRODUCTION

The development of seaplanes for long ranges with a useful load assuring economical flight, has not led to a satisfactory result so far. The difficulties lie in various spheres. The problem of economical long-range flight and its obstacles, has already been treated exhaustively from different points of view. One fundamental obstacle to a satisfactory solution of the long-range seaplane is the take-off. The hydrodynamic processes on its float system set an upper limit to the flying weight which when exceeded leaves the airplane still capable of staying aloft but unable to take off.

In the endeavor to utilize the limits that have been set, to the utmost, with due regard to the load, a knowledge of the physical processes at take-off and the determination of the forces and moments, are imperative. Now the means by which one obtains this information in ship and airplane design, is by testing models, as a mathematical treatment is in most cases impossible. The testing of models of seaplane-float systems is intended to serve two purposes: the development of suitable forms of floats and the determination as exactly as possible of the forces and moments for use in performance calculations. The first problem will not be discussed further in this report.

It has been known for a long time that in the application of the results from tests of models, sources of error exist, the elimination of which may become of decisive importance, especially in the case of the airplanes mentioned above. The endeavor to learn the true magnitude of these errors in research on models and on the basis of this knowledge to correct subsequent model tests, led to the measuring of the forces actually produced in full-scale experiments and the comparing of them with the results from model tests.

The intention to extend such full-size experiments to include seaplane-float systems, is of many years' standing. The first experiments with geometrically similar float models of different sizes in Germany, were those made by Herrmann (reference 1) in collaboration with the DVL and the HSVA in 1926, with a view to determining the effect of the model size on the test data. A continuation of similar investigations followed in 1929 by the DVL at the Hamburg Tank. Subsequently the HSVA carried on the test program independently and also the experiments on full-size floats.

These tests showed that with the test equipment then available, it was not possible to make a correct and complete investigation of a full-size float system whose dimensions corresponded to those of average-size seaplanes. This conclusion was the cause of making the measurements on the seaplane itself rather than in the towing tank.

II. EXPERIMENTATION

1) Structure of Experimental Airplanes

The condition of motion of an airplane-float system is determined by the speed relative to the water v, the trim

α, and the load A. The latter is a function of the water speed, the air speed, angle of attack, propeller thrust, and the aerodynamic properties of the air structure that is attached to the float system. The behavior of a float system is definitely dependent on the properties of this air structure attached to it. Consequently, in the making of model tests that are intended to give a general picture of the behavior of a float system, it is necessary to make the load variable within the practical ranges under consideration as well as the trim and speed.

This requirement governed the construction of the experimental airplane - a Junkers F 13 (fig. 1) - particularly as regards the arrangement of the float system. This was so designed that the float to be investigated lies in the center, below the fuselage. The forces were measured on a three-component balance mounted between airplane and float. Two side floats, attached to the wings, provide the necessary lateral stability as well as a partial unloading of the central float. This is necessary in order to be able to suit the loading of the float to the instantaneous conditions which, as already pointed out, depend upon the effect of the air structure on the float. From this circumstance follows the need for providing an additional unloading, especially in the investigation of models of large flying boats since the latter have, as a rule, a lower get-away speed than the experimental airplane.

Out of consideration for the stability and maneuverability of the machine as well as the strength of the wings, the track of the stabilizing floats was restricted. For the investigation of the effect of interference on the flow, a model of the float system was tested in the towing tank, and the resistance of the central float for different tracks of the stabilizing floats was measured and compared with the resistance without side floats. It was established that with the present track the departures from the unaffected resistance lie within instrumental accuracy.

The changing of the load on the central float was accomplished by increasing the distance of the side floats from the wing by lengthening the flotation-gear struts, so that the load distribution between central and side float could be changed. Since, in this manner, the change of load takes place by steps only and for this purpose the airplane must be lifted out of the water, the three-component balance between airplane and central float was also made adjustable to suit the height, which was accomplished without steps by

means of threaded spindles and can also be done while afloat.

2. Test Equipment

The three-component balance consists of a system of levers, by means of which the forces are conducted to three hydraulic capsules, the hydrostatic pressure in which is a measure of the magnitude of the force acting on each capsule (fig. 2).

The measurement of load, resistance, and trimming moment is done by measuring three components of the resultants, of which two are parallel to the vertical axis, the other parallel to the longitudinal axis. The float is joined to the airplane by two parallel links P_1 and P_2 which receive only the two components N_1 and N_2 parallel to the vertical axis and falling in the direction of the links. For instrumental reasons, the forces occurring at the points of attachment are reduced by levers H_1 and H_2 and led to the capsules M_1 and M_2. The component T perpendicular to the direction of the links is led by a lever H_3, which is pivoted at point O, to capsule M_3. The links and capsules are secured to the main girder S.

The entire three-component balance can be rotated around point B, and thus the angle of setting between float and airplane can be changed. The lever system is of welded-steel tubing; all moving parts are mounted in self-aligning ball bearings.

The capsules are double-acting since negative force components may occur. The capsules (fig. 3) consist of a double piston K sliding in a guide F. The force is applied to the trunnions P of the piston. Both faces of the piston rest on rubber membranes M, which seal the fluid chambers R_1 and R_2 and which make it possible to put the fluid in the capsule under pressure, according to the amount of force acting and the surface of the piston. The pressure leads to the manometers are attached at A_1 and A_2.

The speed is measured by a Prandtl pitot tube located about 70 centimeters below water surface. The method of operation is as follows (fig. 4): There are two leads from the pitot tube to the measuring devices - one for the total pressure on the head, the other for the static pressure on the circular slot. The fluid systems are separated by two rubber membranes M_1 and M_2. On the one side is the meas-

uring fluid; on the other, sea water. The membranes separate the two liquids, although they still permit direct pressure transfer.

Before the taking of a reading, sea water is sucked up by means of a hand pump until the membrane capsules are completely filled. This forestalls any influencing of the indicated pressure by the height of the water column due to the dynamic pressure existing for the time being in the total head line, which is not measurable. The total measuring range is divided between two manometers of different sensitivity. The fine recording instrument is protected against overloading by an automatic cut-off valve V, which closes the pressure line of the fine measuring device on reaching a certain pressure. The trim is recorded photographically. Since the airplane always moves in a horizontal plane during the measurements, it suffices to photograph the shore line simultaneously with a reference on the airplane by a camera mounted in a fixed position on the airplane. The camera was a Zeiss Ikon-Kinamo with a Tessar lens of 4 centimeters focal length. A cross hair fitted in the camera served as reference line.

Systematic preliminary tests made it possible to perfect the recording method so that the force components could be measured within ±0.3 percent accuracy. The capsules were calibrated directly by weight loading. The design of the three-component balance permitted only the measurement of the components lying in a system of body axes. In order to carry out the mathematical determination of the quantities, load and resistance related to the ground axes, it is necessary to know the angle between the two systems of axes, which in the present case equals the angle of trim of the float. The error in the measurement of the trim must not exceed 1/20 degree if the error in the resistance determination under otherwise unfavorable conditions is not to exceed ±1 percent. The photographic record of the trim assures this degree of accuracy. The pitot tube used for measuring the speed was calibrated on the airplane itself by taxying over a staked-off distance at different speeds and comparing the pressure reading with the clocked speed. The calibration curve (fig. 5) with the measured points shows a mean accuracy of about ±1.5 percent of the dynamic pressure. The departure from the theoretical dynamic pressure (dashed lines in fig. 5) is attributable to the effect of the streamlined tube to which the pitot tube was fastened.

All instruments are housed in the cabin of the airplane (fig. 6). The test readings are recorded photographically on standard film with a Zeiss Ikon-Kinamo. The manometers are mounted on an elastically supported board to which the camera is rigidly attached by struts. This camera is synchronized with that used for measuring the trim by a common drive from an electric motor.

Various auxiliary equipment had to be provided - among others, a supplemental system of sea-water cooling for the engine.

3. Test Procedure

For the investigation of scale effect a float was chosen, the form of bottom of which had distinctive characteristics. In these tests only the form of the bottom was of importance, and to save expense the above water form could be made very simple. Accordingly, wooden construction was adopted.

The model used in the investigation was a float with 135° bottom dihedral and a recurved chine. The lines are shown in figure 7.

The actual tests were made on Lake Constance. The measurements were so evaluated that resistance W and trimming moment M_{st} were obtained versus speed and trim for three different load curves. These load curves are derived by means of the equation

$$A = G_o \left(1 - \frac{v^2}{v_{st}^2}\right)$$

where A is the momentary weight on the water (= water lift), v = speed, v_{st} = speed of get-away, and G_o initial load (= ststic buoyancy at $v = 0$). The three different curves of weight on water were obtained by arbitrary choice of G_o and v_{st}.

For the determination of the scale effect two models of the float, at 1:2.5 and 1:5 scale, were tested in the towing basins of the HSVA (Hamburg) and the VWS (Berlin) to determine the mean load curve with due regard to Froude's model law.

4. Choice of Reference Quantities for the Comparison

The question of mechanical similarity is discussed in more detail in a subsequent section (III,2). It may be conceded in advance that the comparison of the test data from different-size models of the same family actually compares processes which are not mechanically similar. Strictly speaking therefore no geometrical similarity exists either. It is therefore a matter of expediency which quantities shall be used as a basis of comparison. In the practical testing it was found expedient to represent the condition of motion of the float system by five quantities: load A, resistance W, trimming moment M, speed v, and trim α. It will be equally expedient to compare those of the quantities which afford a definite picture of the scale effect either for the analysis of the hydrodynamic processes or for the practical application of the model tests. The choice of speed and load on the basis of Froude's law already gives two quantities as a basis for the comparison. The resistance is ruled out because the effect of scale on it is most vital in practical applications. Thus trimming moment or trim must be selected as the third reference quantity.

With one exception, the trimming moment is not a suitable quantity for the analysis of the hydrodynamic changes in condition, for the reason that, consisting as it does of a product force × lever arm, it is not single-valued. If the scale effect on the trimming moment for α = const., or on the trim for M = const., is presented, the magnitude of the scale effect depends not only on the scale of the model but also on the axis of moments selected. There is for every condition a reference axis for which the scale effect on moment or trim disappears altogether. So, to assure clearness, the position of the resultant at α = const. rather than the trimming moment must be compared. This can be accomplished as follows: Choose the reference axis for the trimming moment as nearly as possible in such a manner that the partial moment of the resistance component is small in comparison with the partial moment of the component of the weight on the water; that is, as nearly as possible on the line of action of the resistance component. Then the intersection of the resultant with the line of action of the resistance is the "center of pressure" as in a wing, expressed by

$$h = \frac{M_{st}}{A}$$

The line connecting the step corners was selected as a suitable position of the reference axis because there these assumptions are very closely approximated.

Using this axis, the partial moments of the resistance are small compared to the partial moment of the weight on the water, since this latter is a multiple of the resistance and the movement of the line of action of the resistance is always small. But inasmuch as the weight on the water itself is used as a basis of comparison and so has the same magnitude when comparing two conditions, the comparison of the trimming moments M_{st} of itself indicates with sufficient accuracy the relative magnitude of the scale effect on the simple idea of the "center of pressure position" h. The choice of this reference axis has the further advantage that the plotting position of the center of pressure h affords a measure for the change in pressure distribution due to the scale effect.

In view of these facts, A, v, and α were employed as the basis of comparison, and W and M_{st} were compared. The inverse of the lift/drag ratio, or planing number $\epsilon = W/A$, is also included in the comparison since it provides a criterion for the hydrodynamic efficiency of the float system, just as the center-of-pressure position h for judging the scale effect on the pressure distribution.

5. Effect of Air Loads

The comparison of the test data is disturbed by the effect of the air loads on the float. Because of the experimental technique, it is not possible to provide identical conditions as regards air loads in the full-scale and the model tests. In the former the air loads on the float are included in the measurements; it may be assumed that these air loads are almost those of the free-moving float because the effect of the air structure of the experimental airplane on the air flow can be only insignificent. The effect of the vertical component of the air loads is negligible compared to the load of the float system, so that only the effect of the air resistance and air-trimming moment need be considered. In model tests two different methods were used to neutralize the effects of the air loads on the drag and trimming moment. The one used by the VWS (Berlin) consists in measuring the air resistance at different trims while the raised model is towed just above the level of the water. This method is quite inaccurate because the air resistance of a float that is

taking off partly in the water is different from that of a float towed over the water. In fact, the aerodynamic trimming moment cannot be measured at all by this method. The HSVA (Hamburg) method consists in measuring only the water resistance by fitting a wind screen immediately before the model, extending down to the very edge of the water. From the point of view of the hydrodynamical engineer, this method is undoubtedly the best although even here there is a source of error in the effect on the water spray which, however, can have no great effect on the test result.

To assure a comparison of the test data to which exception could not be taken, the aerodynamic loads were measured in the wind tunnel with due allowance for the influence of the water surface. This test method is not quite exact since the effect of the boundary layer of the plate and of the waves that actually form on the surface of the water cannot be taken into account. Even so, the result of the tests shows that this inaccuracy has no effect on the final result of the comparison. The results of the wind-tunnel tests were applied by subtracting the measured air resistance and the trimming moment from the full-size test data. Similarly, in the model tests of the VWS (Berlin) there was subtracted from the total drag the amount obtained as a result of the over-water towing test. It is to be presumed that the discrepancies between the VWS and the HSVA tests can be traced to too great errors with these methods.

6. The Results of the Comparison

The test data are presented in figures 8 to 19. The VWS tests have been included on the W and M_{st} curves for comparison, although the comparison itself should be restricted, for reasons previously explained, to the full-size test of the DVL and the HSVA measurements. For plotting drag and moments the trim α was selected as parameter. The plotting of the planing number ϵ and of the center of pressure h was confined to the DVL and HSVA measurements, and specifically against the trim α for different speeds. These angles included $\alpha = 3^\circ$, 4°, 5°, 6°, and 7° because an adequate number of test values is available for these.* Plotting the values of W and ϵ shows the effect of the scale on the size of the horizontal component of the resultant, those of M_{st} and h,

*For lack of space, only the values for $\alpha = 3^\circ$, 5°, and 7° are reproduced here.

the effect of the scale on the location of the resultant at the float and on the pressure distribution.

Resistance: The ascending branch of the W curves discloses the peculiar fact that the 1:2.5 size model has the highest, and the 1:1 size float the lowest resistance, and the differences at $\alpha = 3^\circ$ are somewhat greater than at 4°. In towing tests of ship models, it has also been observed occasionally that the results from small models of less than 1-meter length are in closer agreement with those from large models over 5 meters long than the results from medium-size models of about 2.5-meter length (reference 2). At around $v = 5.8$ meters per second and small trim, the curves fork into two branches. The lower branch shows, in the range $v = 6$ to 9 meters per second, a slower increase in resistance, while with the 1:1 size float, there is even a brief decrease in resistance at $\alpha = 3^\circ$ and $v = 8$ m/s. The sequence of the curves starting from $v = 6$ m/s is 1:5, 1:2.5, 1:1, with 1:1 having the lowest resistance. Beginning at $v = 8.5$ m/s, the resistance increases very rapidly. The curves for the three scales are here practically alike. The maximum resistance lies between $v = 10.5$ and $v = 11$ m/s. The position of the curves is such that the 1:1 float has the lowest, the 1:5 the highest resistance. As α increases the difference diminishes somewhat. In the first part of the descending branch of the curve this sequence remains at first as far as $v = 13.5$ m/s, to be followed by an irregular shape of the 1:2.5 and 1:5 curves, which at times even undercut curve 1:1. In this range also can be seen the tendency to minimum resistance for the 1:1 scale float, and that the difference decreases as α increases. At high speeds the curves for the 1:2.5 and 1:5 models show a marked rise in resistance again, which commences the sooner the greater the trim. This is due to the fact that the afterbody touches the water again and the resistance therefore becomes greater. This was not observed on the 1:1 model where, to be sure, these running conditions were not measured at $\alpha = 7^\circ$.

Planing number ϵ: Naturally the scale effect must reveal the same tendency as the resistance curves themselves. The diagrams reveal that the 1:1 float has almost always the best ϵ; the curves further permit the determination of the best trim for any speed.

Moment of trim M_{st}: With exception of the curves $\alpha = 3^\circ$ the moment curves are coincident up to around

$v = 9.5$ m/s. Only in the zone where two regimes of flow are possible, as already discussed in connection with the resistance curves, greater divergences occur. This suggests that in this critical zone of partial flow separation the viscosity has a greater effect. The maximum moment values occur at the same speeds as the maximum resistance values. The scale effect produces a decrease in moment as the size of the model increases. This tendency persists up to about $v = 14$ to 15 m/s, where a partial overcutting of the curves occurs, attributable to inadequate instrumental accuracy at small trimming moments.

Center of pressure h: The tendency of the scale effect must, of course, be the same as for the plotting of M_{st}. At speeds beyond $v = 16$ m/s the values become too inaccurate for comparison.

III. THEORY

1. Mechanical Similarity (reference 3)

Complete agreement of processes in the model test with the conditions encountered for full size is obtained only when complete mechanical similarity exists between both processes. This is predicated on the assumption that all physical forces affecting the flow are in the same ratio to the inertia forces.

In bodies moving on the boundary surface of two mediums of different densities, the viscosity and gravity forces are of primary importance in the flow phenomena. From the derivation of these force correlations follow the laws of similarity:

$\frac{\text{Inertia forces}}{\text{Viscosity forces}}$ = const., the Reynolds law of similarity,

and $\frac{\text{Inertia forces}}{\text{Gravity forces}}$ = const., the Froude law of similarity.

These laws of similarity give the equations of the conditions under which a model test must be made if mechanical similarity of phenomena is to exist between model and full size, not only as regards inertia forces but also as regards one of the other types of forces mentioned.

The laws of similarity state that for the viscosity forces the Reynolds Number

$$R = \frac{v\,l}{\nu}$$

and for the gravity forces the Froude Number

$$F = \frac{v}{\sqrt{gl}}$$

must be equal for model and full size.

Considering the viscosity forces, if the medium for model and full size is the same, the product of model length × velocity must be constant; i.e., if the geometrical dimensions of the model and of full size are in the ratio of λ the speeds in the model test must have the λ^{-1} times value, while as regards the gravity forces the speeds must have the $\lambda^{1/2}$ times value. This is the reason why no combined consideration of inertia and gravity forces is possible - as long as the same medium is employed for both the model and full size.

This has led to making model tests in which the flow phenomena are affected by viscosity as well as gravity in such a way that in the test itself the gravity forces are taken with consideration because experimentally it is easier to comply with the Froude than with the Reynolds model law. The disregard of the viscosity forces leads to discrepancies in the flow form and hence in the test results, which are designated as "scale effect," whose size depends upon the scale of the model and on the proportion of the viscosity forces to the total process. In naval design the viscosity is taken into account mathematically by determination of the friction forces on the basis of measurements of the resistance of flat plates at the same Reynolds Numbers. This method presupposes a knowledge of the wetted surface, the wetted length, and a friction coefficient.

Quite apart from the errors ensuing from this method in the conversion to full size, it is not applicable to planing water craft because the wetted area as well as its length is, according to the conditions of motion and loading, subject to large fluctuations and can therefore not be utilized for computing the frictional resistance. On that account the frictional forces have been disregarded heretofore in such cases and work has been confined to reaching

the Reynolds Number for full size by using the largest possible models and high towing speeds, which led to the building of high-speed towing carriages in the Naval Experimental Laboratories.

2. The Physical Causes of Scale Effect

The disregard of the viscosity forces in model tests may affect the form of the flow in two ways: 1) through the influence of the surface friction on the boundary-layer conditions and so on the tangential forces; 2) through influencing the pressure distribution and the normal forces. Both effects are of course intimately related because of their common origin.

a) Influencing the tangential forces.- The relation between frictional resistance and Reynolds Number has been exhaustively investigated in plate and pipe tests. It was found that for the boundary layer, three forms of flow are possible: laminar, turbulent, and turbulent with laminar approach. The results of the tests are shown in figure 20. For the flat plate the shear stress at point x in laminar flow is derived from the theory of the boundary layer according to Blasius (reference 4):

$$\tau_l = 0.664 \frac{\rho}{2} v^2 \left(\frac{vx}{\nu}\right)^{-1/2} \qquad (1)$$

in turbulent flow with the aid of the test data (reference 5) as

$$\tau_t = 0.0576 \frac{\rho}{2} v^2 \left(\frac{vx}{\nu}\right)^{-1/5} \qquad (2)$$

From these the friction coefficients are derived as

$$C = \frac{K}{\frac{\rho}{2} v^2 F} = \frac{2}{\rho v^2 l} \int \tau \, dx \qquad (3)$$

for laminar flow as

$$C_l = 1.327 R^{-1/2} \qquad (4)$$

and for turbulent flow as

$$C_t = 0.074 R^{-1/5} \qquad (5)$$

In turbulent flow with laminar approach the coefficient is formed from the two parts for the laminar and the turbulent and consequently depends upon the point of transition from laminar to turbulent condition. Therefore, C may be written as

$$C_f = \frac{K}{\frac{\rho}{2} v^2 F} = \frac{2}{\rho v^2 l} \left[\int_0^{l_k} \tau_l \, dx + \int_{l_k}^{l} \tau_t \, dx \right] \qquad (6)$$

in which l_k is the point of transition from laminar to turbulent flow and l = the total length of the plate. According to Gebers (reference 6), this transition takes place on a smooth flat plate at a critical Reynolds Number of $R_k = \sim 5 \times 10^5$. The introduction of this value and of the coefficients cited in (4) and (5) into equation (6) gives, according to Prandtl (reference 7), the coefficient for turbulent boundary layer with laminar approach as

$$C_f = C_t + \frac{l}{R} \left[1.327 \, R_K^{1/2} - 0.074 \, R_K^{4/5} \right] \qquad (7)$$

$$C_f = 0.074 \, R^{-1/5} - \frac{1700}{R} \qquad (8)$$

The critical Reynolds Number obtained from Gebers' experiments and employed by Prandtl is, strictly speaking, applicable only to flat, smooth plates in a longitudinal flow. The transition to turbulent flow can also occur at some other Reynolds Number. The reasons are: the effects of roughness of the surfaces, the effect of the pressure distribution on a three-dimensional form (in contrast to a flat plate in a longitudinal flow), the turbulence of the medium already existing upstream from the body, and the vibrations of the body in the fluid. Given the particular critical Reynolds Number, the corresponding coefficient can be computed according to equation (6). Figure 20 shows the friction coefficients versus Reynolds Number for various critical Reynolds Numbers. The limits are defined by the fact that R_k is reached just at the trailing edge of the plate (purely laminar flow) or already exists at the leading edge (purely turbulent flow). Taking $R_k = 5 \times 10^5$ as the upper limit, beginning at which the boundary layer is in any case turbulent, the diagram reveals that within a large range of Reynolds Numbers entirely different coefficients are possible, depending upon the

external circumstances cited above. This knowledge makes it possible to explain the experimental results in which the data for small models are in better agreement with the data from large models than are the data from medium-size models, which has been already pointed out in section II,6 in the discussion of the results from the tests. At larger Reynolds Numbers all coefficients approach those of pure turbulent flow; the friction forces become independent of the external influences that are decisive in the critical range because the preponderant part of the boundary layer is turbulent and no longer appreciably influenced by the minor influence of the laminar entrance length. In the following, several possibilities for the magnitude of the coefficient of friction will be discussed by means of a numerical example.

Let the full size have a wetted length $L = 2$ meters at a speed of $v = 15$ meters per second. The Reynolds Number is obtained for $\nu = 10^{-6}$ (for warer at $t = 20^{\circ}$ C. temperature) as

$$R_{1:1} = 3 \times 10^{7}$$

For the 1:5 size model, the corresponding Reynolds Number at identical Froude number is

$$R_{1:5} = \lambda^{3/2} R_{1:1} = 2.68 \times 10^{6}$$

Assuming a critical $R_k = 5 \times 10^{5}$ the coefficient of friction for the full size is

$$C_{1:1} = 2.31 \times 10^{-3}$$

1) How large is the friction coefficient for the model?

Assuming equal R_k the friction coefficient for the model is

$$C_{1:5} = 3.20 \times 10^{-3}$$

that is about 38 percent greater than for full size.

2) How large would the critical Reynolds Number for the model have to be to make the coefficient of friction the same for both the full size and the model?

$$R_k = 8.45 \times 10^{5}$$

This value is practically unobtainable because in Gebers' experiments $R_k = 5 \times 10^5$ appeared to be probably the upper limit.

b) Effect of the normal forces.- Another effect appears as the result of the change in pressure distribution caused by the viscous forces, although this may occur because of a change in the separation phenomena as well as because of a change in the pressure distribution in regions of adhering flow. Separation phenomena are produced when because of the slowing up of the fluid in the boundary layer by friction the particles of fluid suffer a loss of kinetic energy and then are no longer able to penetrate into a region where the pressure is higher. The point, then where the piling up and separation from the boundary of this slowed-up fluid takes place, depends on various factors:

1) On the pressure distribution along the boundary, steep pressure rise favors separation.

2) On the time rate of flow - in retarded flow separation is easier.

3) On the structure of the boundary layer. A movement of the point of separation may be associated with the change from laminar to turbulent condition and because of it the distribution of pressure on the body may be radically changed.

4) On the condition of the surface. If the boundary layer on a smooth surface is perfectly laminar, roughening the surface can cause it to become turbulent at the same Reynolds Number. The effect described under 3) can likewise occur because of it. But, if the flow in the boundary layer is already turbulent, an increase in roughness will always result in an increase in the friction coefficient as seen in figure 20, which shows, in addition to the coefficients for flat plates, the coefficients (reference 8) for various degrees of relative roughness k/l (k = grain size) obtained from the Göttingen pipe experiments and properly converted to apply to plates.

The change in pressure distribution through a shift in the front of separation is especially pronounced when the proportion of the separation (eddy) resistance is great compared to the frictional (tangential) resistance

and when the point of separation has not been previously established by the use of a very full form or by sharp chines and steps. But planing seaplanes have, for the purpose of effecting the separation of flow from a part of the body and through it obtaining a decrease in resistance, one or even several transverse steps, so that for them the position of the front of the separation is fixed by constructive measures. For this reason the scale effect as a result of the shifting of the front of the separation, has no particular significance as far as they are concerned, in contrast to ships and the rounded bodies used in airplane design. For this reason also, the attempts by any method to induce artificial turbulence in the boundary layer in model tests are unsuccessful in model tests of airplane-float systems. Among such methods are the fitting of a "turbulence wire" or a local roughening on the model, or even the towing behind turbulence screens or grids. These are always followed by an increase in the friction coefficient. By influencing the location of the point of separation, however, this can, in ships and rounded bodies lead to a drop in the total resistance because of the decrease in eddy resistance and so make for a better agreement between full-size and model tests.

As yet little is known regarding the influencing of the pressure distribution in regions of adhering flow. But that such must exist is proved by the test data. The change in the position of the center of pressure h or in the trimming moment M_{st} can only be the result of a shift of the resultant, because with the reference axis that was used the effect of the changed frictional (tangential) force is almost eliminated.

3. Order of Magnitude of Scale Effect

From the investigation of the physical causes, it is also possible to draw conclusions as to the order of magnitude. We shall now investigate only whether the experimental data can be explained as to direction and order of magnitude on the basis of these considerations.

The order of magnitude of the possible differences in friction coefficient between full size and model can be estimated when the Reynolds Numbers are known. It is to be noted that the coefficients given in figure 20 cannot be directly applied to the conditions existing on the float, because the distribution of pressure and velocity is unlike that on the plate.

A further obstacle exists in the calculation of the Reynolds Number. In the airplane-float system the determination of the "wetted length" as well as of the true speed of the water over the planing bottom, present some difficulty. The comparison of the experimental results with the plate friction coefficients is therefore merely a more or less inexact determination of the order of magnitude. Since the conditions in the buoyant condition are quite complicated, only an example from the purely planing condition will be considered here. In the planing condition the wetted length is a part of the length of the planing bottom which, however, varies rapidly and especially, for the V-type planing bottom is not definite. A key to the wetted lengths of the planing bottom is found from observation during model tests or from plotting the "center of pressure position" h. During the planing-surface tests at the HSVA (reference 9), it was determined that the position of the center of pressure and the wetted length preserved an almost constant relation.

Making this assumption for the V-bottom float, from the plotting of h it is possible to estimate the wetted length approximately. In the model tested, the pure planing condition was reached at around $v = 13$ meters per second. The length of the wetted planing bottom was then approximately $L = 1.0$ meter (at $\alpha = 5^{\circ}$* trim). This gives a Reynolds Number of $R = 1.0 \times 10^7$, and accordingly, $R_{2.5} = 2.53 \times 10^6$ and $R_5 = 9 \times 10^5$ for the models. It should be borne in mind that these Reynolds Numbers change as a result of the effect of the temperature on the kinematic viscosity of the water. The difference between model and full-size tests amounts to about 30 percent, since the latter was made at an average temperature of around 20° C., against about 10° C. for the model test.

---

*The length of the planing bottom was obtained as follows: The ratio, according to the planing surface-tests (reference 9) is:

$$\frac{\text{Position of center of pressure}}{\text{Wetted length}} = 0.8$$

Figure 18 gives for $v = 13$ m/s and $\alpha = 5^{\circ}$ the center of pressure $h = 0.8$ m, whence the wetted length is computed as $L = \frac{h}{0.8} = 1.0$ m.

So in the example selected, under the assumption $R_K = 5 \times 10^5$ the Reynolds Numbers and the friction coefficients are the following:

Model	1:1	1:2.5	1:5
R =	1.3×10^7	2.53×10^6	9×10^5
C_f	2.74×10^{-3}	3.31×10^{-3}	2.98×10^{-3}

The magnitude of the frictional resistance for the full size is:

$W_R = W - A \tan \delta$ (δ = angle of attack of planing bottom).

For $\delta = 6^0$, A = 1,015 kg, W = 165 kg

$$\underline{W_{R_1} = 58 \text{ kg}}$$

Taking into consideration the calculated friction coefficients, the frictional resistance for the 1:2.5 scale model is

$$W_{R_{2.5}} = \frac{C_{f_{2.5}}}{C_{f_1}} W_{R_1}$$

$$\underline{W_{R_{2.5}} = 70 \text{ kg}}$$

and for the 1:5 scale model

$$\underline{W_{R_5} = 63 \text{ kg}}$$

This means an increase in resistance of 21 and 9 percent, respectively. The experimental results for this example show that the order of magnitude between full scale and the 1:2.5 model is in agreement. But they also show that the model test at the 1:5 scale was made in a range of Reynolds Numbers in which the coefficients are profoundly affected by the critical Reynolds Number and may exceed or even fall below the coefficient for the 1:2.5 size model. This is probably also the reason for the intersection of the two model curves in planing condition. From the plotting of the position of the center of pressure h it appears that the wetted length decreases as the speed in-

creases. Consequently, the rough assumption can be made that the approximate size of the Reynolds Number changes inappreciably during planing. It also explains why, in planing, the resistances of the full-size model are invariably less than for the 1:2.5 model, while those of the 1:5 model at large trim angles fall still lower, because in the range of Reynolds Numbers in which the full-size and 1:2.5 model lie, no appreciable changes in the coefficient can take place.

The effect of the scale on the pressure distribution is seen from plotting M_{st} or h. Obviously, as the model increases in size, the resultant shifts toward the step. This is in agreement with the HSVA planing-surface tests (reference 10) where, on the basis of measurements of the wetted surface it was pointed out that that result should not be attributed to a shortening of the wetted length but rather to a change in the pressure distribution.

For the investigation of the agreements of the approximate size of the scale effect with the pressure distribution we shall use the same example as in the study of the frictional resistance. For comparison the previously quoted planing-surface tests are utilized - with the assumption, however, that the conditions are not materially changed, even under greater variations of load. The planing-surface tests were made for a step loading of A/b^3; that is, about half of that used for the sample problem. The floats then correspond approximately to the following scales of the surfaces used in the planing-surface tests:

Full-size	1:1	= surface	2:1
Float	1:2.5	= surface	1:1.25
Float	1:5	= surface	1:2.5

It may be assumed that the effects of the scale on the "moment coefficient" C_m from the planing-surface tests and on the "position of the center of pressure" h considered in this report are of the same magnitude.

The planing-surface tests yielded the following scale effect:

Approximately	17	percent	between	1:1	and 1:2.5
"	36	"	"	1:1	" 1:5

and from the comparative data with float III:

About 14 percent between 1:1 and 1:2.5

" 25 " " 1:1 " 1:5

The result of these calculations shows that the results of the comparison between DVL full-size and model tests are in good agreement as regards both direction and approximate size with the theoretical argument as well as other test data, considering the partially rough assumptions.

In view of this fact, the scale effects resulting from the conversion of the model tests to the largest seaplane-float systems in existence can be calculated. The Reynolds Numbers for the float that was investigated and the largest float system designed up to the present , are approximately as 1:6. The comparative model with 1:2.5 length scale represents the upper limit for the available test equipment in naval-research laboratories. As a rule the model tests are made with smaller models of the order of size of about 1:4 to 1:5 of the float that is being investigated. For those sizes the ratio of the Reynolds Numbers is about 1:50 to 1:70. In this case the ranges in which the planing conditions fall for the float considered as an example, both for model and full size, occur at about

$$R = 9 \times 10^5 \text{ to } 1.3 \times 10^6 \text{ for the model}$$

and $R = 8 \times 10^7$ for full size (Do X, for instance)

From figure 20, it may be seen that the friction coefficients for the model, if smooth surfaces be assumed, may fluctuate between

$$C_f = 3 \times 10^{-3} \text{ and } 4.5 \times 10^3$$

depending on the effect of the laminar zone, while the coefficient for full size is invariably

$$C_f = 2 \times 10^{-3}$$

According to that, the possible scatter in frictional resistance may in such cases mount to 75 percent of the value for the full size. Since this scatter in the example considered would involve a possible error in total resistance

of around 25 percent $\left(\text{at } \frac{W_R}{W} \approx \frac{1}{3}\right)$, it is advisable when investigating airplanes of such sizes to accept the greater expense and the experimental difficulties which are involved in the use of models of the size of the comparative model (1:2.5). In this case the Reynolds Number would lie at around 2.5×10^6; that is, in a region within which the possible scatter because of the laminar effect is substantially less. Even so, the safety of an estimate of the scale effect would be still greater in this case than when small models were being used, although the friction coefficient ($C_f = 4 \times 10^{-3}$) is about twice as large as for full size.

IV. APPLICATION TO ACTUAL PRACTICE

It was pointed out in the Introduction that the exact determination of the resistance is of major importance for heavily loaded long-range seaplanes. In order to show the working out of results from full-size tests in practice, the following example will illustrate the effect of an inaccurate determination of the resistance in a model test:

Based upon the data from full-size and model tests, the take-off times and distances were computed for an airplane with different thrust loadings and plotted in figures 21 to 23 against the initial thrust loading S_o/G_o.

The simplifying assumptions made for the airplane were as follows:

1. The resistance of this float system at any speed is the minimum, irrespective of whether the air structure can produce the corresponding trimming moment.

2. Unloading is assumed according to the square law in accordance with the unloading schedule chosen for the model comparison without consideration of the changes in trim during the take-off.

3. Increase of the air resistance W_L of the whole airplane is assumed according to the square law.

The initial thrust loadings selected S_o/G_o correspond to the following conditions:

$$\frac{(S - W_L) - W}{W} = \frac{\text{accelerating force}}{\text{float resistance}}$$

at the maximum resistance of the full size:

$$\frac{S_o}{G_o} = 0.1625 \quad 0.1750 \quad 0.1875 \quad 0.200 \quad 0.2125$$

$$\frac{S - W_L - W}{W} = 0.071 \quad 0.160 \quad 0.249 \quad 0.342 \quad 0.431$$

Figures 22 and 23 further show the comparatively poorer take-off time and distance compared to the full size. The result of this study is the following:

In airplanes with large excess of power the scale effect is small; for example, at $S_o/G_o = 0.21$ and 1:5 model, it amounts to about 10 percent increase in take-off time and run. For heavily loaded airplanes with small excess of power, the results are otherwise. Take-off times of 50 seconds and more are normal for such airplanes. The error from the use of the 1:2.5 model test data amounts in this case to about 60 percent in take-off time and to about 48 percent in take-off run, while for the 1:5 scale model, it already amounts to ∞.

One fortunate feature, however, is that the conditions for the full size are more propitious, hence it may be assumed that failures in the take-off performance because of scale effect, will not occur in seaplane design.

The most important result of the tests is the perception that for reasonably safe determination of the take-off performances, models must be used of sizes comparable to the comparative model of 1:2.5 scale. It is only with models of such sizes that one reaches the supercritical range.

Translation by J. Vanier,
National Advisory Committee
for Aeronautics.

REFERENCES

1. Herrmann, H., Kempf, G., and Kloess, H.: Tank Tests of Twin Seaplane Floats. T.M. No. 486, N.A.C.A., 1928.

2. Weitbrecht: Über den Masstab-Einfluss bei Modell-Schleppversuchen. Vortrag vor der Schiffbautechn. Gesellschaft, November 1932.

3. Weber: a) Die Grundlagen der Ähnlichkeitsmechanik und ihre Verwertung bei Modellversuchen. Jahrbuch der Schiffbautechn. Gesellschaft, 1919, S. 355.

   b) Das allgemeine Ähnlichkeitsprinzip der Physik und sein Zusammenhang mit der Dimensionslehre und der Modell-Wissenschaft. Jahrbuch der Schiffbautechn. Gesellschaft, 1930.

4. Blasius, H.: Grenzschichten in Flüssigkeiten mit kleiner Reibung. Z. f. Math. u. Phys., Bd. 56 (1908), S. 1.

5. Ergebnisse der Aerodynamischen Versuchsanstalt zu Göttingen I. Lieferung, S. 121.

6. Gebers: Das Ähnlichkeitsgesetz für den Flächenwiderstand im wasser geradlinig fortbewegter, polierter Platten. Schiffbau, 1921.

7. Ergebnisse der Aerodynamischen Versuchsanstalt zu Göttingen III, Lieferung, S. 4.

8. Hydromechanische Probleme des Schiffsantriebes. Veröffentlichung der Vorträge der Konferenz, 1932, S. 90.

9. Sottorf, W.: Experiments with Planing Surfaces. T.M. No. 661, N.A.C.A., 1932.

10. Sottorf, W.: Masstabversuche mit Modellschwimmern des Typs HSIH und Gleitflächen. HSVA-Bericht vom 4. July 1931.

11. Garner, H. M., and Coombes, L. P.: The Determination of the Water Resistance of Seaplanes. R. & M. No. 1289, British A.R.C., 1929.

12. Garner, H. M.: Seaplane Research. Jour. Roy. Aero. Soc., vol. 37, 1933, p. 830.

Figure 1.- Experimental Junkers airplane F13 with DVL three-component balance.

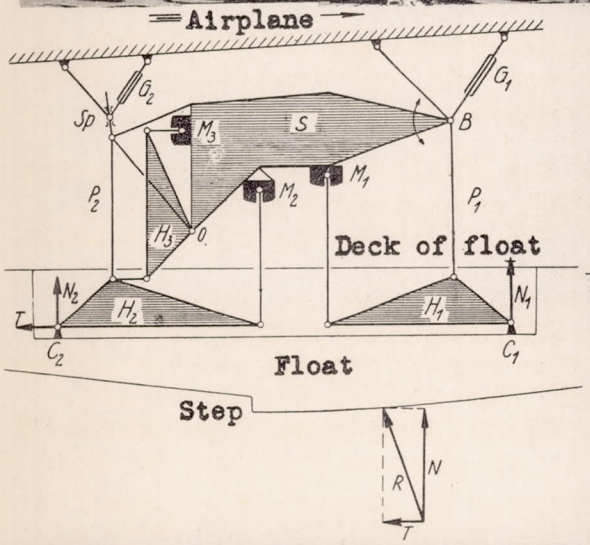

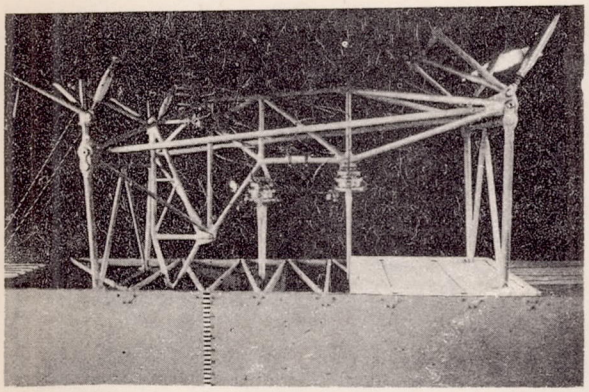

B Pivot of three-component balance
C_1, C_2 Points of attachment to the float
G_1, G_2 Threaded spindles for adjusting the distance of the float from the airplane
H_1, H_2, H_3 Levers. M_1, M_2, M_3 Capsules
O Pivot of H_3. P_1, P_2 Strut frames
Sp Spindle regulating incidence
S Main girder. R Resultant
N_1, N_2 Normal force components
T Tangential force components

Figure 2.- Diagram and side view of the DVL three-component balance.

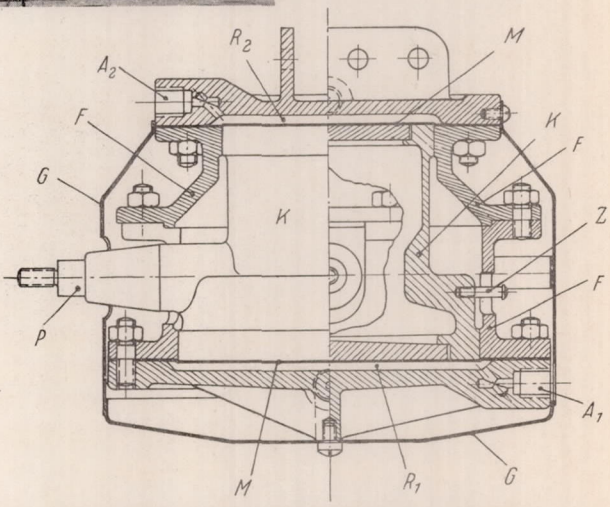

A_1, A_2 Pressure line connections
F Guide of the piston. G Housing
K Double piston. M Rubber membrane
P Trunions for application of force
R_1, R_2 Fluid chambers
Z Indicator for making the position of the piston visible

Figure 3.- Hydraulic double capsule for the DVL three-component balance

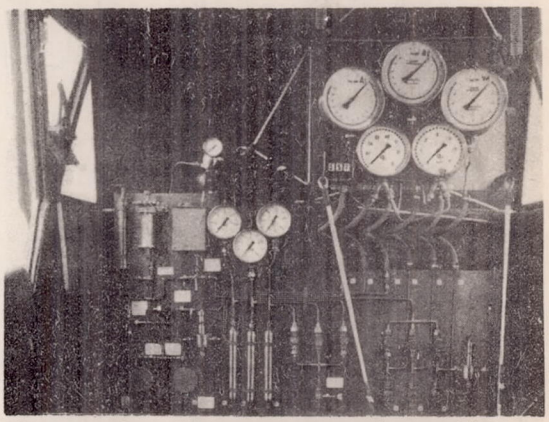

Figure 6.- Measuring and auxiliary instruments mounted in the cabin of the experimental airplane.

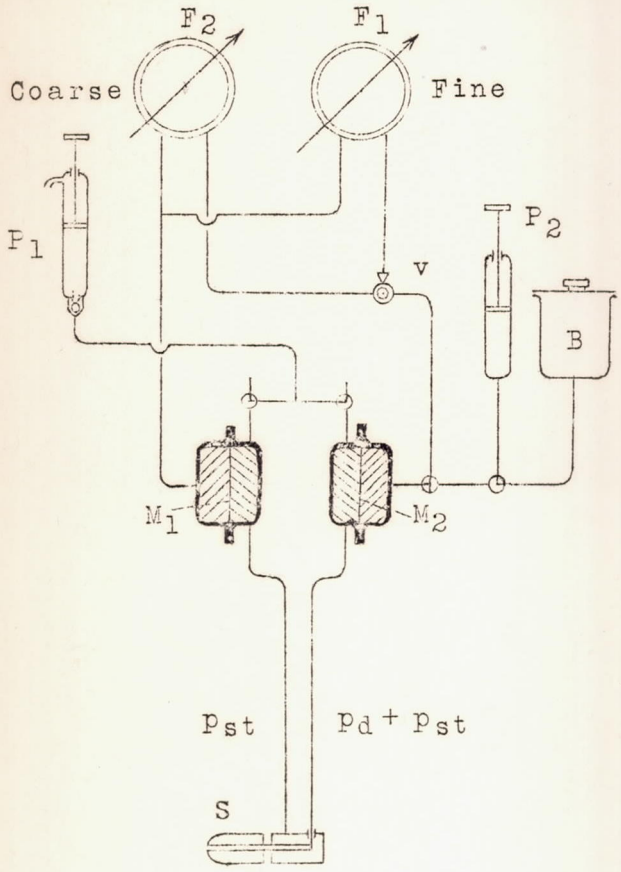

B	Tank for fluid
F_1 F_2	Manometers
M_1 M_2	Rubber membranes
P_1 P_2	Pumps
p_d+p_{st}	Total head
p_{st}	Static pressure
S	Prandtl pitot tube
v	Safety valve for fine manometer

Figure 4.- Diagram of the dynamic pressure recording unit with under-water pitot tube.

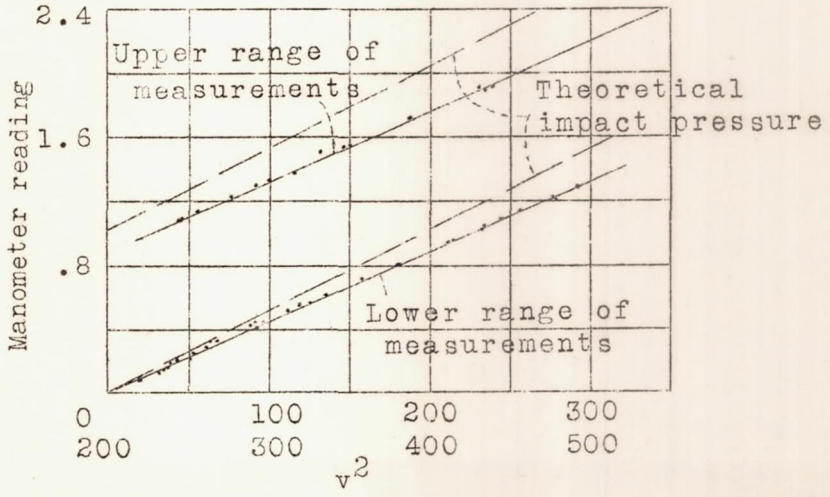

Figure 5.- Calibration curve of under-water pitot.

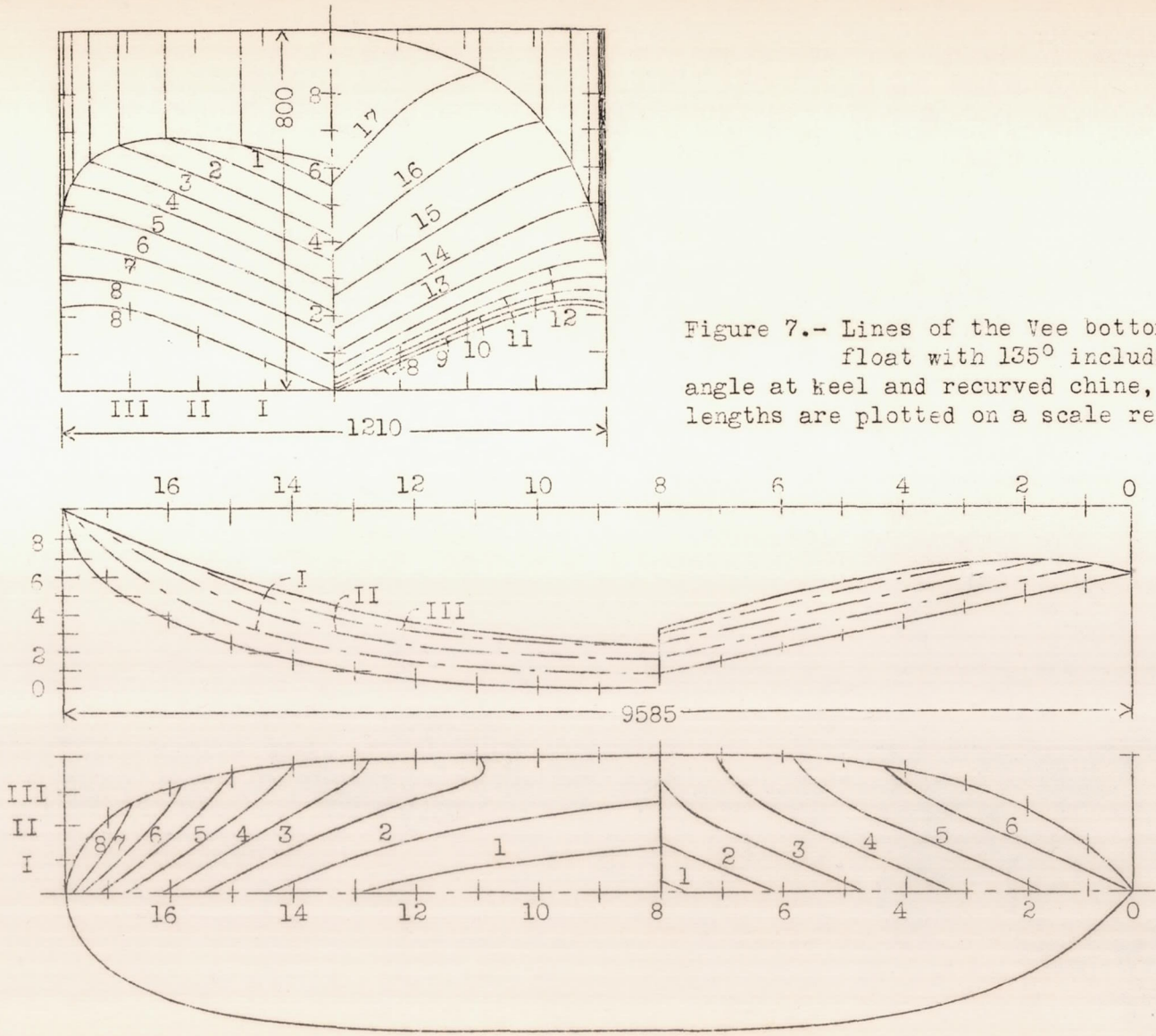

Figure 7.- Lines of the Vee bottom float with 135° included angle at keel and recurved chine, the lengths are plotted on a scale reduced 1:2

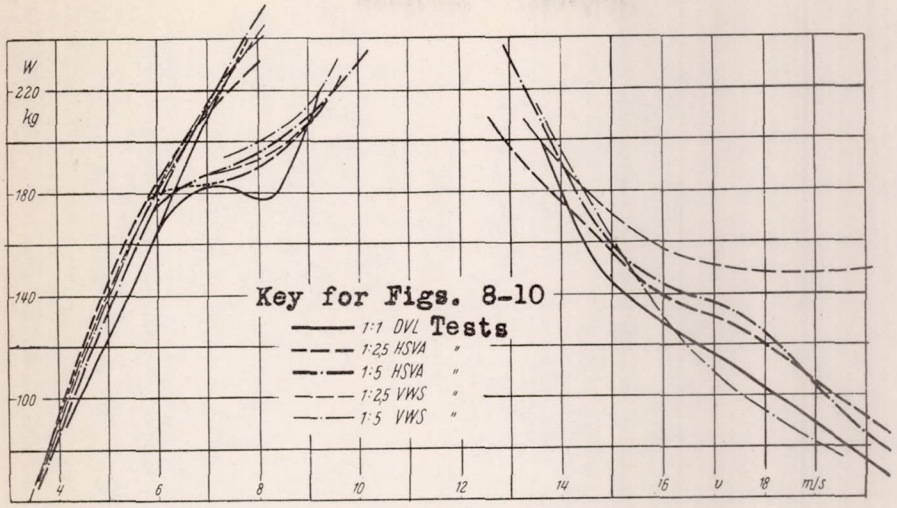

Figure 8.- Resistance W at $\alpha = 3^{\circ}$

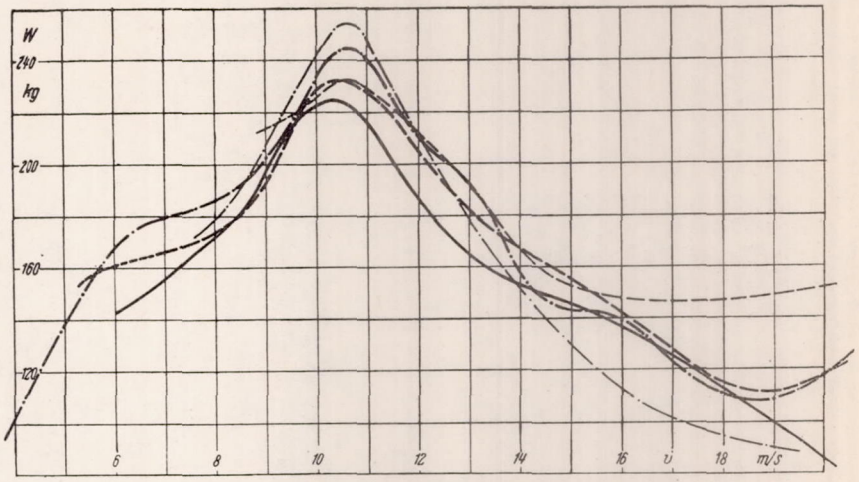

Figure 9.- Resistance W at $\alpha = 5^{\circ}$

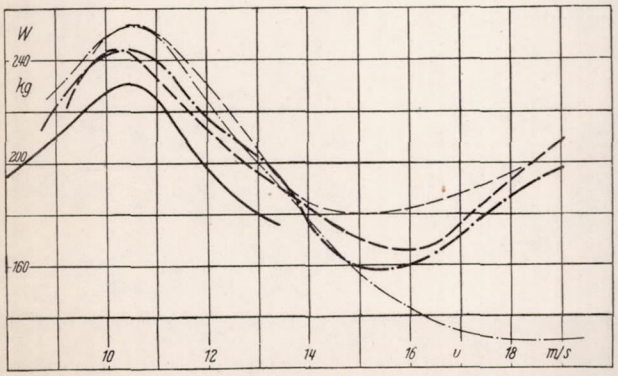

Figure 10.- Resistance W at $\alpha = 7^{\circ}$

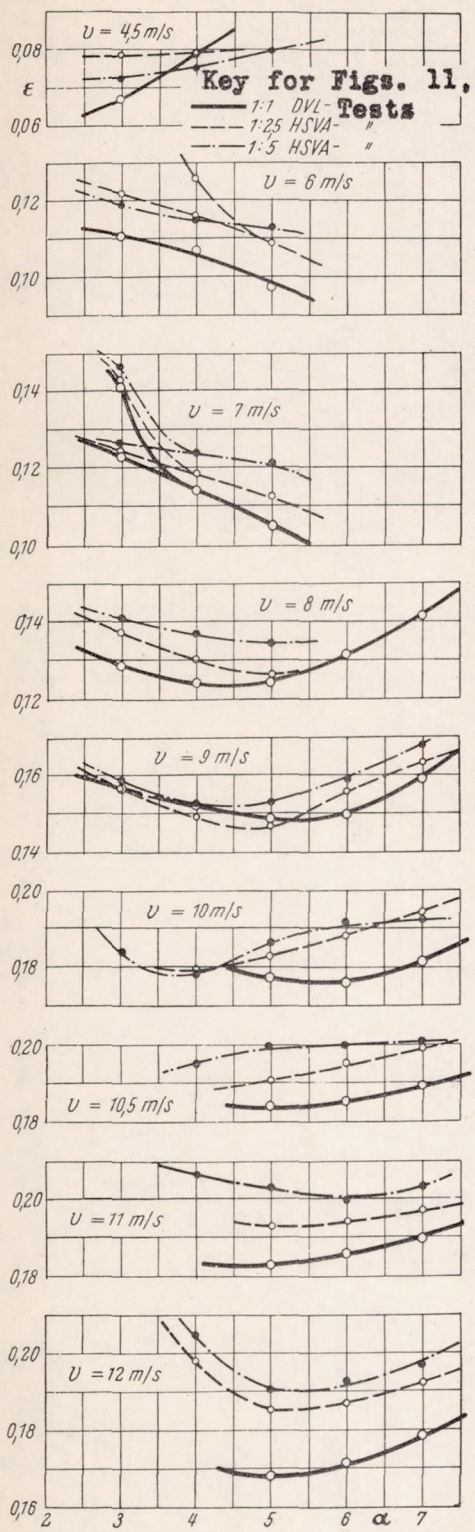

Figure 11

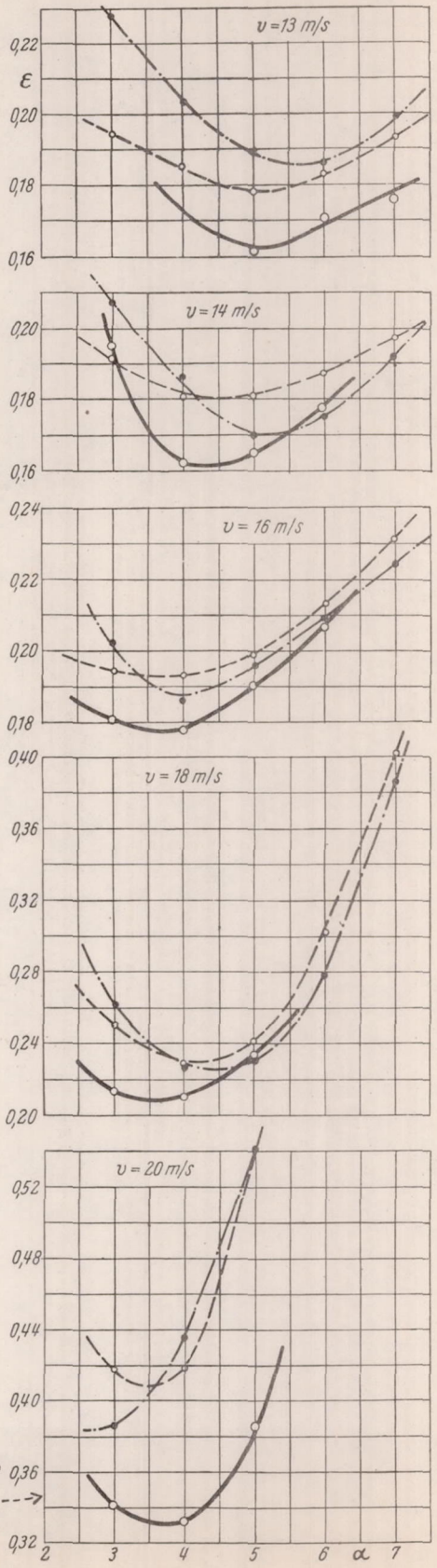

Figure 12

Figures 11,12.- Planing number $\epsilon = W/A$ for $v = \text{const.}$

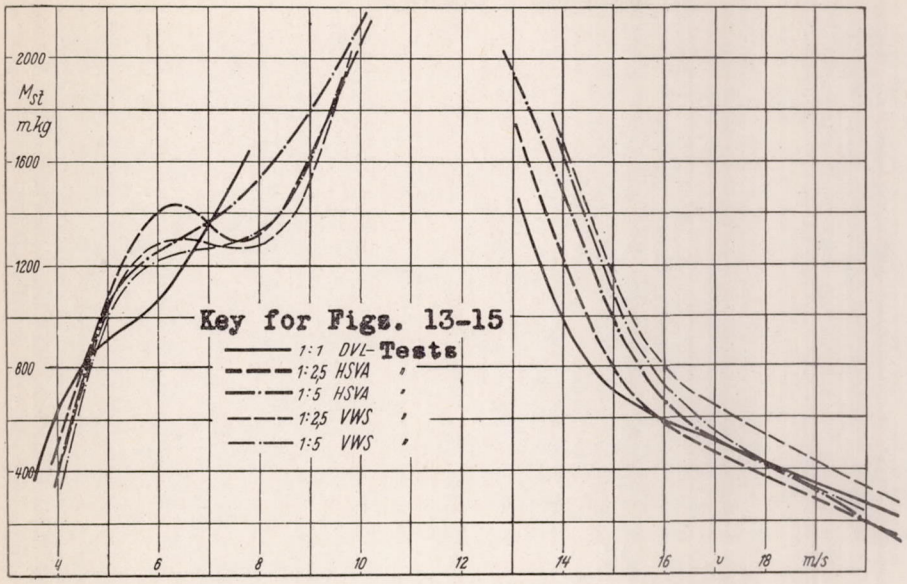

Figure 13.- Trimming moment M_{St} at $\alpha = 3^{\circ}$

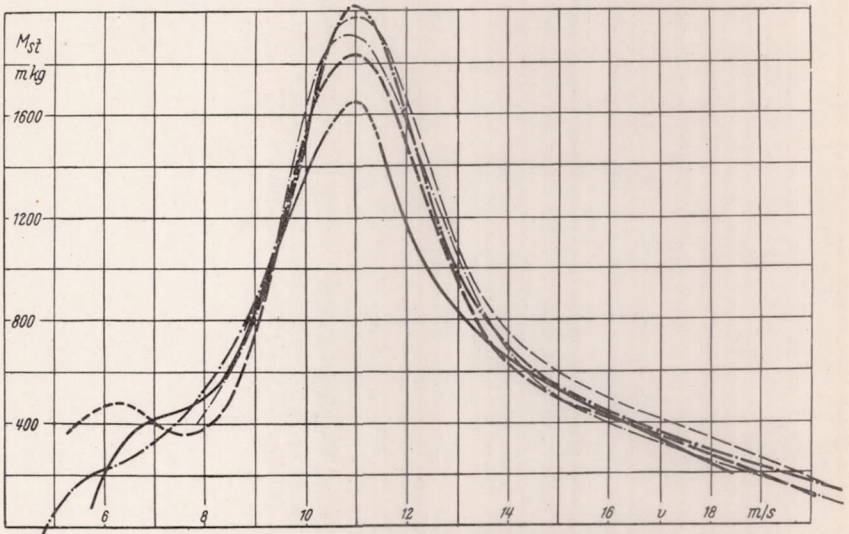

Figure 14.- Trimming moment M_{St} at $\alpha = 5^{\circ}$

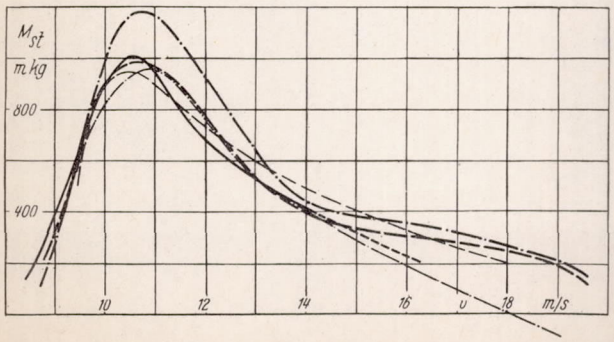

Figure 15.- Trimming moment M_{St} at $\alpha = 7^{\circ}$

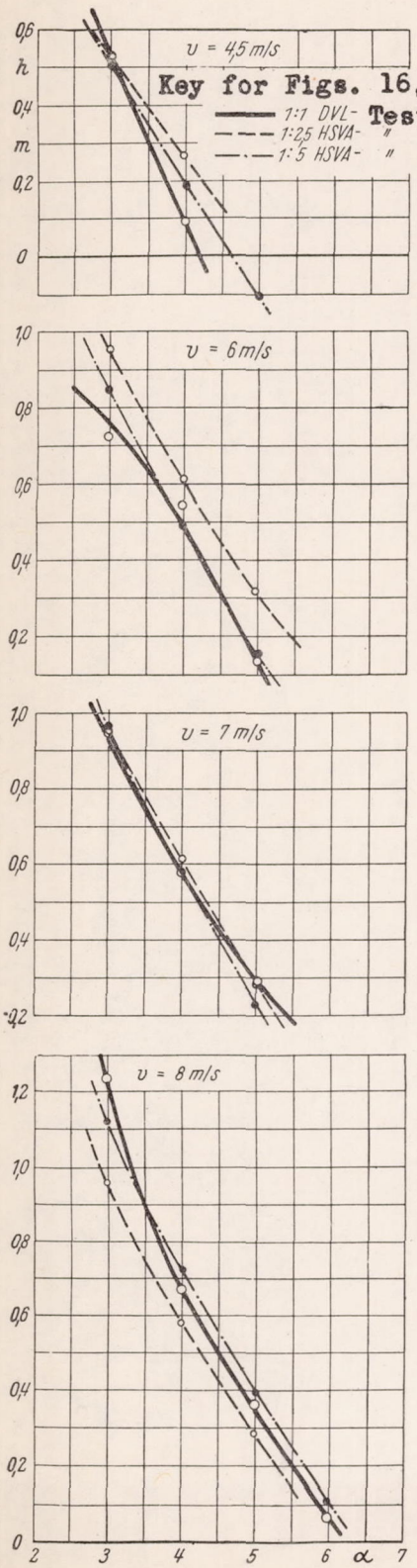

Figure 16

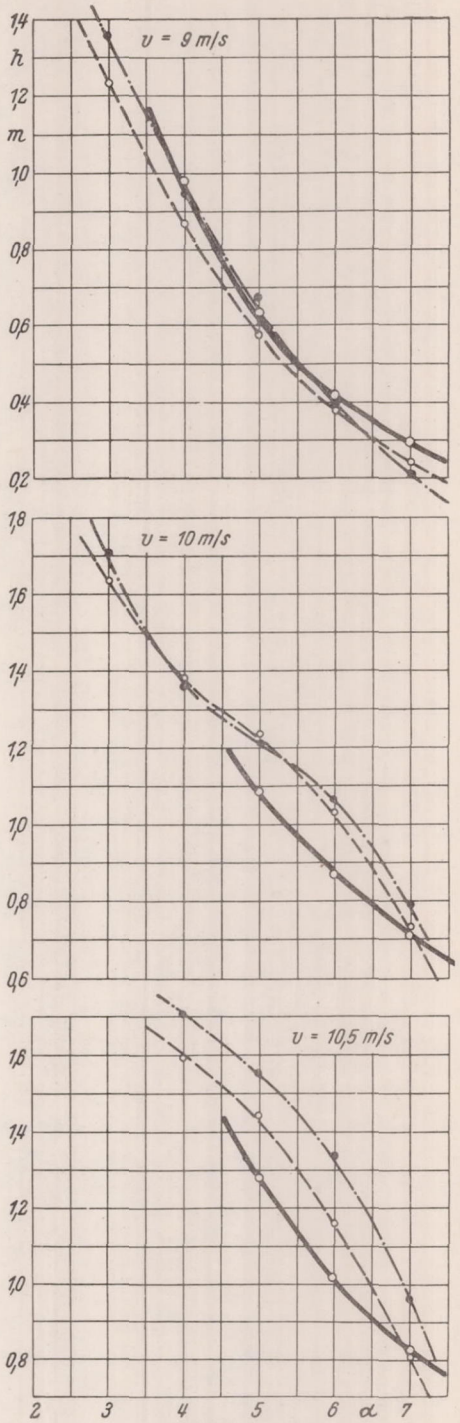

Figure 17

Figures 16,17.- Position of center of pressure
h = Mst/A for v = const.

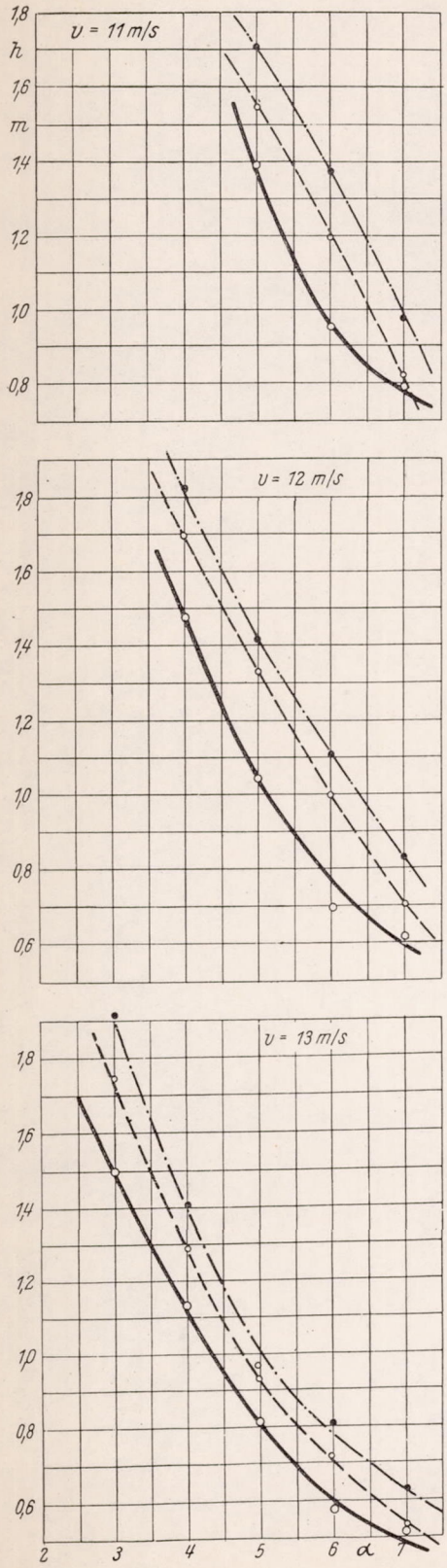

Figure 18

Key for Figs. 18,19

1:1 DVL Tests
1:25 HSVA "
1:5 HSVA "

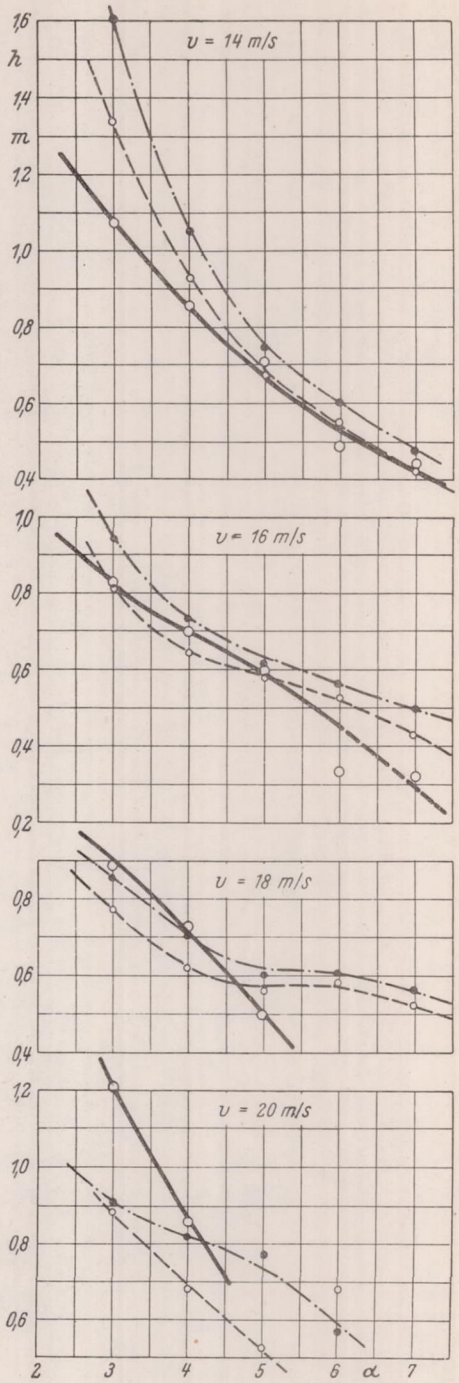

Figure 19

Figures 18,19.- Position of center of pressure
$h = M_{st}/A$ for v = const.

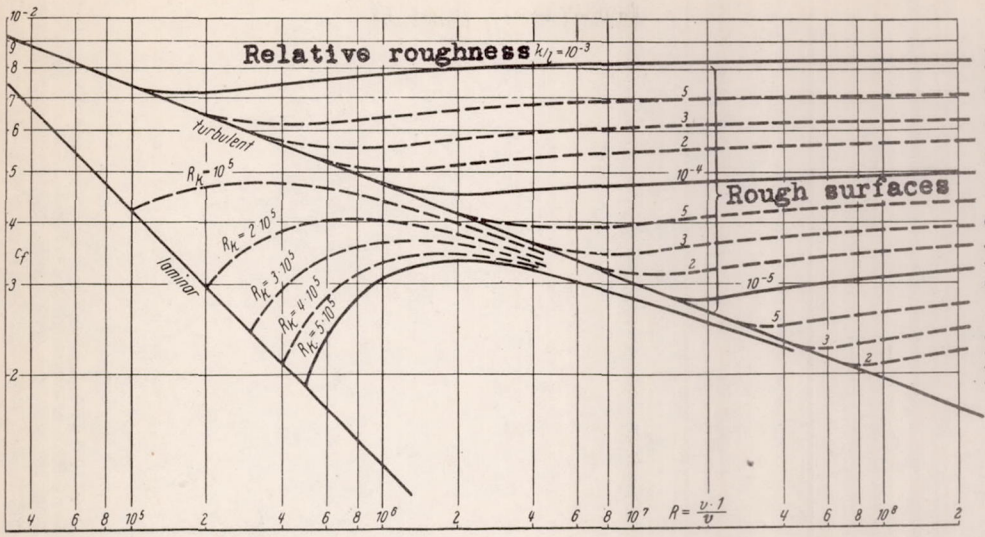

Figure 20.- Coefficients of friction for smooth and rough plates at different critical Reynolds Numbers

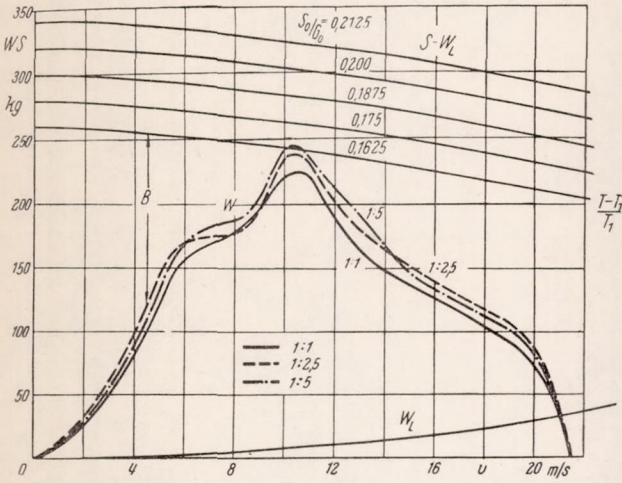

Figure 21.- Examples showing the variation of the forces during the take-off of a seaplane with different thrust loadings.

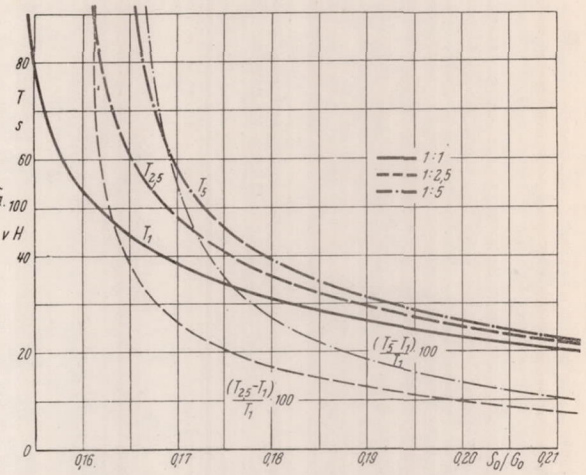

Figure 22.- Take-off time and increase of take-off time compared with the take-off time of the full size.
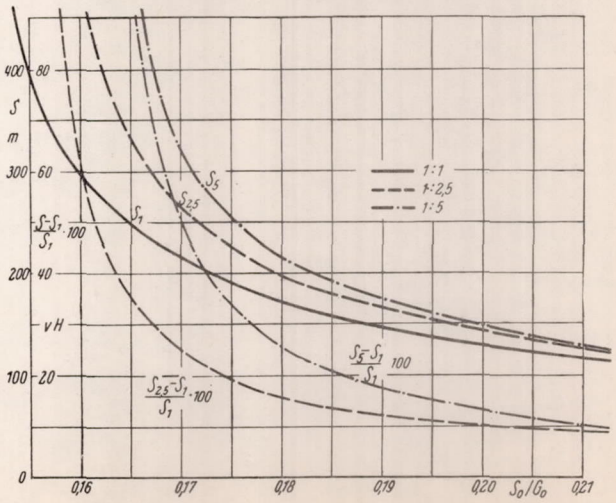
Figure 23.- Take-off run S and increase of take-off run compared with the take-off run of the full size.